Jour. Petrol. Soc. Korea
Vol. 5, No. 1, p. 1~9, 1996

The use of fluid inclusions to constrain P-T-X conditions of formation of Eonyang amethyst

K. H. Yang

Department of Geology, Pusan National University, Pusan, 609-735, Korea

ABSTRACT : Eonyang amethyst deposits are thought to be spatially and temporally associated with the biotite granite of the Kyeongsang Basin. The examined euhedral quartz crystals in cavities in the aplite intruded biotite granite are colored-zoned from white at the base to amethystine at the tops. Three types of primary inclusions were observed and three isochores for inclusions representing each types are constructed to constrain the trapping conditions and fluid evolution involved during the formation of the amethyst. The intersection of the isochore representing the early fluid inclusions with solidus temperature of the host granite indicates initial quartz formation at about 600℃ and 1.0-1.5 kbars. Intermediate quartz formation, associated with the high-salinity inclusions, occurred at somewhat lower temperatures (400℃) and pressures of about 1 kbar. The amethystine quartz formed from H_2O-CO_2-NaCl fluids at temperatures between 280-400℃ and pressures of about 1 kbar. Early quartz is interpreted to have formed from fluids that either exsolved from or were in equilibrium with the granite at near solidus conditions, whereas the amethystine quartz apparently grew from fluids of at least partial sedimentary origin.

Key words : primary inclusions, trapping condition, isochore

INTRODUCTION

The Eonyang amethyst mining district is located in the Cretaceous Kyeongsang basin in the southeastern part of the Korean peninsular (Fig. 1). The amethyst deposits produce some of the highest quality amethyst in Korea (Kim *et al.*, 1988). These amethyst deposits associated with the Cretaceous-early Tertiary granite (referred to locally as the Eonyang granite) of the Kyeongsang Basin contain abundant miarolitic cavities indicating the presence of fluids during late-stage crystallization of the granite.

Several workers (Kim and Moon, 1984; Kim *et al.*, 1988; Yang *et al.*, 1994; Youn and Park, 1994) have examined fluid inclusions in the amethyst and granite. They showed consistent homogenization temperatures ranging from 130℃-540℃ and salinities up to 58 wt.%. However, many uncertainties remain concerning their interpretation. Yang *et al.* (1994) suggested that the minimum pressure of amethyst formation is at least higher than 600 bars based on the homogenization temperature of fluid inclusions trapped in the upper part of the amethyst. In addition, the pressure of amethyst formation was estimated to be less than 72 bars based on the evidence of boiling during inclusion formation (Youn and Park, 1994).

The present study focused on the amethyst from miarolitic cavities in an aplite dike and presents data on the formation temperature and pressure, compositions of fluid inclusions, and the evolution of fluid properties attending amethyst formation. These data were obtained from petrographic, Raman spectroscopic and microthermometric analysis of the fluid inclusions. Many secondary inclusions also occur along microfractures in the amethyst, but the time relationships between different generations of secondary inclusions could not be established. Thus, only primary inclusions were

examined in this study.

GENERAL GEOLOGY AND PETROGRAPHY OF HOST ROCKS

The studied amethyst deposit occurs in an aplite dike within the biotite granite which intruded middle Cretaceous sedimentary and volcanic rocks of the Hayang formation in the Kyeongsang basin. The Eonyang granite hosting the amethyst deposit is extensively exposed on the western side of the Yangsan fault line in the central part of the Kyeongsang Basin (Fig. 1). K/Ar dating of biotite from the Eonyang granite gives an age of 72 Ma (Lee and Ueda, 1976).

Igneous activity in the Kyeongsang Basin occurred from 120-40 Ma. (Lee, 1972; Min *et al.*, 1982; Lee *et al.*, 1987). Some of the Cretaceous-early Tertiary granitoids of the Kyeongsang Basin represent subvolcanic complexes that intruded terrestrial sedimentary and volcanic rocks comprising the Kyeongsang Supergroup

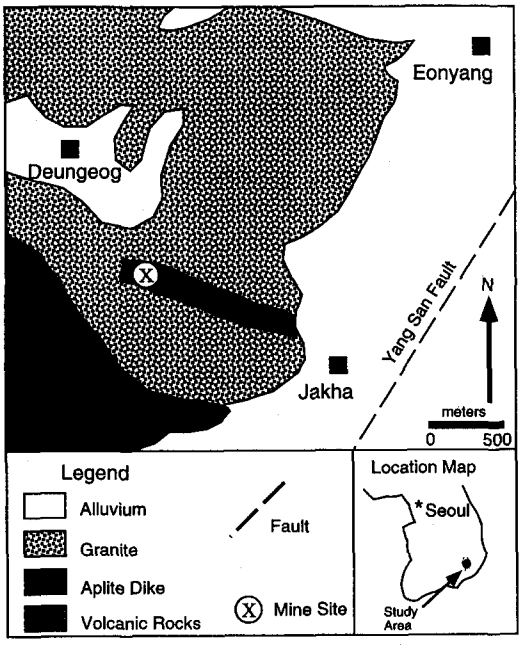

Fig. 1. Location map of the study area showing the amethyst mine (after Lee, 1980). Samples selected for fluid inclusion study were from the open-pit mine.

along NNE trending structures and circular sturctures related to cauldron subsidence. Most of the Cretaceous-early Tertiary granitoids of the Kyeongsang Basin are associated with contemporaneous volcanic rocks ranging in composition from andesite through dacite, rhyodacite and rhyolite. The intrusives occur as batholiths and as small scattered oval and irregularly-shaped plutons, and some intrusives are surrounded by narrow contact metamorphic zones of hornfels up to 2 km wide (Lee, 1972; Chang, 1975; Jin *et al.*, 1981; Lee *et al.*, 1987). Major element geochemistry and isotopic and trace element studies suggested that the Cretaceous-early Tertiary granitoids of the Gyeongsang Basin were rapidly fractionally crystallized from a calc-alkaline andesitic or granodioritic magma which was generated by partial melting of subducted oceanic crust at a compressional plate margin (Jin *et al.*, 1981; Jin, 1985, 1986; Hong, 1987).

The Eyonyang biotite granite exhibits a porphyritic, granular texture and consists of quartz, alkali feldspar, plagioclase, and biotite. Porphyritic alkali-feldspar is often enclosed by reaction rims of plagioclase. Porphyritic quartz grains are highly corroded. Porphyritic subhedral plagioclase generally shows zonal textures with rectangular outlines. Grains are usually subhedral to anhedral showing rapakivi texture and well-developed mialoritic cavities. Opaque minerals include magnetite, hematite, and pyrite. Altered pinkish alkali-feldspar and white quartz crystals are abundant in mialoritic cavities with amethyst and pyrite present in smaller amount.

Most amethyst, including those studied here, is hosted in the aplite dike which intruded the porphyritic biotite granite. Mialoritic cavities, which host large, high-quality amethyst, abundant in the aplite dike, which consists of the same mineral phases as the porphyritic granite. The largest cavities in the aplite dike range up to 150 cm in diameter. Euhedral quartz crystals in the cavities vary in color from white at the base of crystals to clear to

purple at the terminations. The contact between aplite and the white quartz is altered to clay minerals. No alteration or chilled margins were found at the contact between the aplite dike and host granites.

ANALYTICAL TECHNIQUES

Six euhedral quartz crystals from mialolitic cavities in the aplite dike were collected for this study. Quartz crystal showing purple color and observable growth zones were selected to investigate conditions of amethyst formation and variation in fluid properties during crystal growth. The crystals show well-developed growth zones from white quartz at the crystal base to amethyst at the terminations and contain primary aqueous inclusions. Polished plates were prepared for petrographic, microthermometric and Raman analysis to determine the fluid compositions and trapping temperatures of fluid inclusions and to investigate the variations in those features during crystal growth.

Laser Raman Spectroscopy

Laser Raman spectroscopy was used to identify daughter minerals and gas phases in 26 fluid inclusions in the amethyst. Data were obtained using a Dilor XY multichannel spectrometer equipped with a CCD detector (256× 1024 element array) and an Ar^+ laser. An Ar-laser beam with a wavelength of 514.5 nm is focused on daughter crystals and gas phases through 100X objective of a microscope. Solids and volatile phases were identified by comparision of obtained spectra with reference spectra; calcite, carbon dioxide, CH_4, and N_2 were identified.

Microthermometry

Doubly polished sections 0.07-0.1 mm thick were prepared for fluid inclusion microthermometric analysis. Heating and cooling experiments were carried out using a Fluid Inc.-adapted USGS gas flow heating/cooling stage. The stage was calibrated with pure CO_2 (-56.6℃) and pure H_2O (0℃ and 374.1℃) synthetic fluid inclusions (Bodnar and Sterner, 1987). The accuracy and reproducibility of temperatures of phase changes are approximately ±0.1℃ at T≤ 50℃; ±0.5℃ at T≤374.1℃; and ±5℃ at T≤ 573℃. Salinities of gas-free inclusions were calculated using the program SALTY of Bodnar *et al.* (1989); salinities of CO_2-bearing inclusions were calculated from clathrate melting temperatures using the equation of Darling (1991). Isochores for H_2O-NaCl inclusions were calculated using the equations in Bodnar and Vityk (1994), while those for H_2O-CO_2-NaCl incluisons were calculated using the equations of Bowers and Helgeson (1983) in MacFlinCor (Brown and Hagemann, 1994).

RESULTS

Four types of fluid inclusions were observed

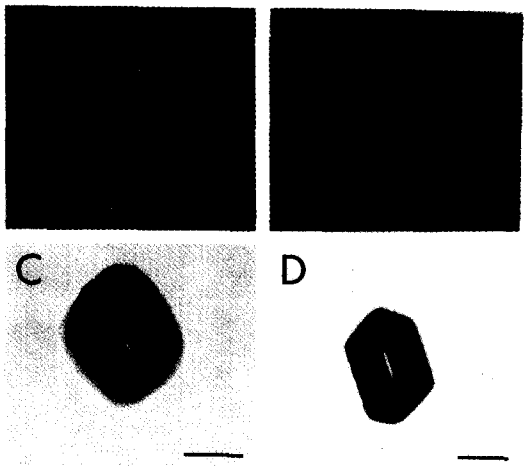

Fig. 2. Photomicrographs of the different types of inclusions observed in the amethyst. The scale bar represents 10 m for each inclusions, and all photographs were taken at room temperature. A. Type I liquid-rich inclusion with calcite daughter minerals. B. Type II halite-bearing inclusion with calcite and opaque daughter minerals. C. Type III CO_2-bearing inclusion in the upper amethystine part of the quartz crystal. The small amount of aqueous solution along the walls are visible. D. Type IV vapor-rich inclusion showing no obvious liquid phase.

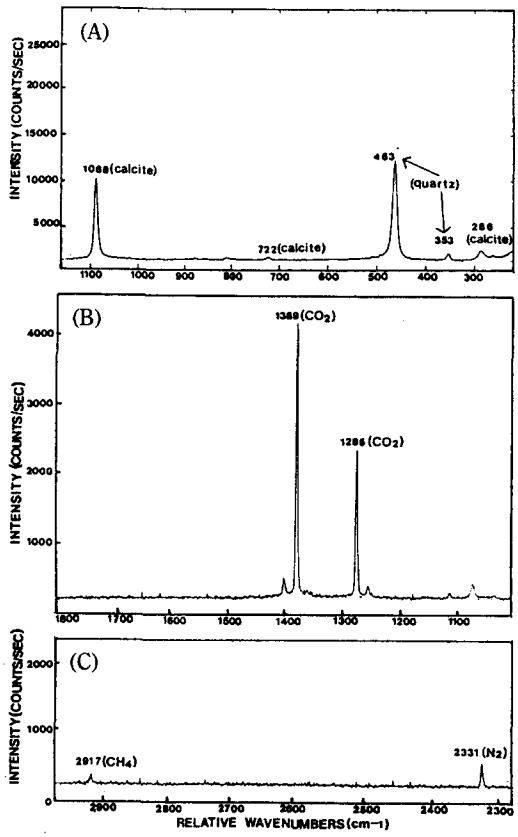

Fig. 3. Raman spetra of (A) calcite and (B) CO_2 and (C) CH_4 and N_2.

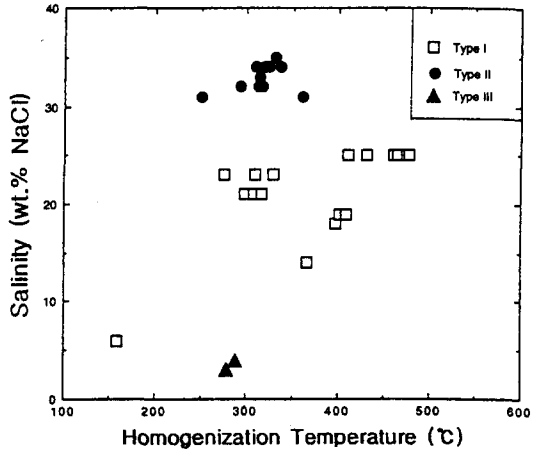

Fig. 4. Homogenization temperatures for type I, II, and III inclusions.

based on room temperature phase behavior; these inclusions are referred to as Types I, II, III, IV and are described below (Fig. 2).

Type I inclusion:

Liquid-rich, low-salinity type I inclusions contain liquid+vapor+daughter minerals other than halite. Vapor bubble occupies less than half the volume of the inclusion at room temperature (Fig. 2A). Primary inclusions of this type always contain calcite and unidentified opaque minerals showing homogeneous phase ratios. Calcite was identified based on the crystal shape, strong birefringence in transmitted light, and characteristic Raman lines at 1088, 722, and 286 cm^{-1} (Fig 3A). Opaque crystals might be sulfides (pyrite?, chalcopyrite?) based on the brassy color under reflected light. Some crystals showing a reddish color and are apparently hematite. Primary inclusions of this type are negative crystal shaped and occur along growth zones in the white quartz. Their size ranges from 20 to 50 μm. Irregular-shaped type I inclusions along fractures are abundant in the white quartz portion of the crystal adjacent to the aplite. They are mostly <3 μm in diameter.

The first noticeable melting temperature of ice in primary type I inclusions was between -32 and -30℃, suggesting the presence of salts other than NaCl, which has a eutectic temperature of -21.2℃ (Hall *et al*, 1988). Melting might have begun as much as several degrees below this temperature. Final melting of ice occurred between -26.2 and -25.1℃, corresponding to salinities of about 24-25 wt. %. (Fig. 4). These salinities were determined using the observed ice-melting temperatures and referring to the extrapolated ice-liquid curve in the H_2O-NaCl system. Primary type I inclusions homogenize between 447 and 480℃ (Fig. 5). Calcite did not disolve during heating.

Secondary type I inclusions sometimes contain CO_2, as evidenced by a noticeable melting event around the vapor bubble in the range -57 to 58℃ and by Raman bands at 1389 and 1285 cm^{-1} (Fig. 3B). A CO_2 clathrate that dissolved at about -3.4 to -4.0℃ (Fig. 6). Final melting

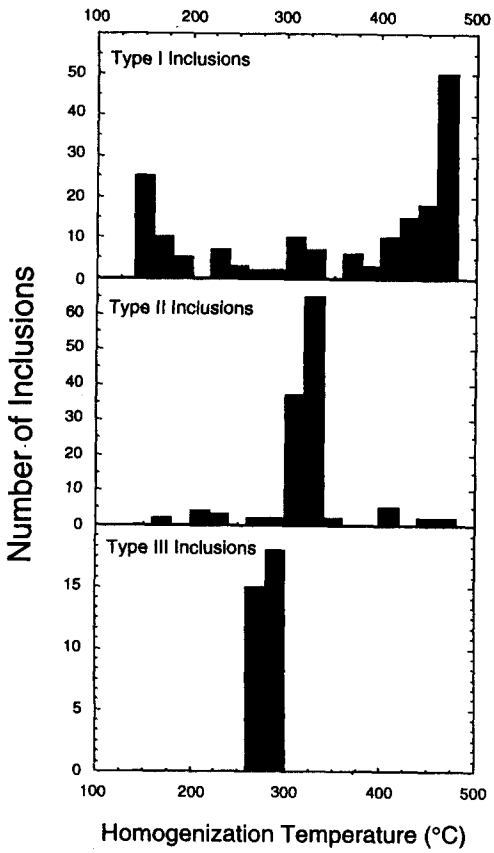

Fig. 5. Relationship between salinity (in wt.% NaCl equivalent) and homogenization temperatures for type I, II, and III fluid inclusions.

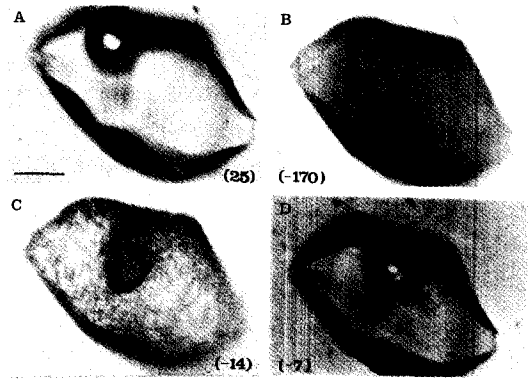

Fig. 6. Photomicrographs showing the formation of ice and clathrate during cooling of type I inclusions. The scale bar represents 20 μm. They are all taken at the temperatures indicated in the parentheses. Temperatures are in degrees Celsius. A. Fluid inclusion contains vapor bubble and liquid at room T, 25℃; B. Deformed vapor bubble and ice at -170℃. Refractive index of the inclusion is changed due to the ice formation. Because of the volume increase (about 9%) of ice, the vapor are deformed. C: Deformed vapor bubble, ice and clathrate at -14℃ showing the intermixed ice and clathrate; D: Liqud, euhedral clathrate crystal, and deformed vapor bubble because of the attached clathrate at -7℃. These clathrate crystals disappeared at -4℃.

of ice occurred at -5.7 to -9.9℃ (about 9-14 wt. % NaCl). The depression of the CO_2, melting point below -56.6℃ is attributed to the presence of CH_4 and N_2, both of which were detected by Raman band at 2917 cm^{-1} and 2331 cm^{-1}, respectively (Fig. 3C). They homogenize between 156-160℃.

Type II inclusion:

This group of inclusions are liquid-rich and contain halite, calcite, and opaque daughter minerals (Fig. 2B). Size varies from 10 to 40 μm. Type II inclusions show a three-dimensional distribution outlining former quartz crystal faces in the white quartz. These inclusions are considered to be primary and were trapped after type I inclusions but before type III inclusions, based on petrographic evidence. Irregularly shaped type II inclusions also occur near the white quartz base of crystals. Type II inclusions do not occur in the upper part of the amethyst crystals.

Halite in primary type II inclusions dissolved at 214-219℃ corresponding to salinities of about 33-34 wt.% NaCl equivalent (Fig. 4). Other daughter minerals, including calcite, did not dissolve during heating runs. The vapor bubbles in type II inclusions disappeared at 320°-333℃ (Fig. 5).

Type III inclusion

Type III inclusions contain liquid CO_2, CO_2 gas, and aqueous liquid at room temperature (Fig. 3C). Inclusion size ranges from about 10 to 80 μm. Liquid CO_2, and gaseous CO_2 occupy greater than 50 volume percent of the inclusion. The presence of liquid and gaseous CO_2 phases at room temperatures indicates that the

pressure of fluid in the quartz bottle are about 50-60 bars at the outcrop. Type III inclusions are generally regular in shape and show a narrow range of CO_2/H_2O volume ratios (70-80%) at room temperature. The uniform phase ratios suggest that these inclusions were trapped from an originally homogeneous mixture of CO_2 and H_2O, i.e. in the one-phase-fluid field. Type III inclusions occur mostly in the amethystine portions of the quartz crystals. This type of inclusion is rarely observed as secondary inclusions in the white quartz near the base of the crystal.

Temperatures of homogenization to the CO_2 phase range from 24°-25℃ to the liquid phase. Total homogenization to the CO_2 ("vapor") phase occurred between 273°-288℃ (Fig. 5). Melting temperatures of clathrate were about 8℃, corresponding to salinities of about 4 wt.% NaCl equivalent (Darling, 1991). Solid CO_2 melted at -57.4° to -57.8℃ in the cooling experiment. Both CH_4 and N_2 were detected during Raman analyses of type III inclusions (Fig. 3C).

Type IV inclusion:

Type IV inclusions are two-phase (liquid+vapor) with the vapor bubble occupying ≥90 volume percent of the inclusion. This type of inclusion occurs mostly along fractures and is of secondary origin. The size ranges from <5 μm to 120 μm. The inclusions show variable shape ranging from negative crystal to irregular. No volatiles (other than H_2O) were detected by Raman analysis. Because of the large amount of vapor and the difficulty of determining the homogenization temperatures of inclusions which homogenize to the vapor phase (Bodnar *et al.*, 1985), no microthermometric data were obtained from this type of inclusion. Some of the secondary vapor-rich inclusions may be associated with liquid-rich inclusions which homogenize at about 85℃, indicating possible fluid immiscibility at low temperature. The homogenization temperatures of the coexisting liquid-rich inclusions and the distribution of the vapor-rich and liquid-rich inclusions along fractures suggest that the type IV inclusions occur as a late feature, and that all vapor-rich inclusions were trapped after formation of the crystal.

DISCUSSION OF RESULTS

The Eonyang amethysts are of high quality, and exploration for new occurrences might benefit from a well-constrained genetic model for their formation. The main question to be asked in this paper concerns the pressure of amethyst formation and how much erosion has occurred since the time of formation to expose the deposits near the earth's surface. If the amethyst is genetically related to the granites and aplite, the pressure of amethyst formation provides additional information concerning the depths of emplacement of the granite.

Youn and Park (1994) concluded that the amethyst was formed at low pressure (72 bars) and at about 300℃ with salinity of 20 wt. % NaCl, based on the fluid inclusion studies. They also suggested that amethysts were formed below 72 bars. These P-T conditions suggest the formation of the amethyst at relatively near-surface, non-magmatic conditions. However, the amethyst deposits occur in an aplite dike and, less commonly, in the host granite. The aplite dike and the coarse-grained host granite have similar composition and mineralogy. Based on this information and field observations, it has been assumed that the aplite dike and the granite are co-magmatic, and that the aplite intruded shortly after emplacement of the granite. There is no evidence of a chilled margin along the boundary between the dike and granite.

Euhedral quartz crystals in cavities in the aplite are colored-zoned from white at the base to amethystine (purple) at the tops. Fluid inclusions with distinctly different compositions and homogenization temperatures occur in the different portions of the quartz crystals. The earliest fluids are represented by primary type I inclusions which occur along growth zones in

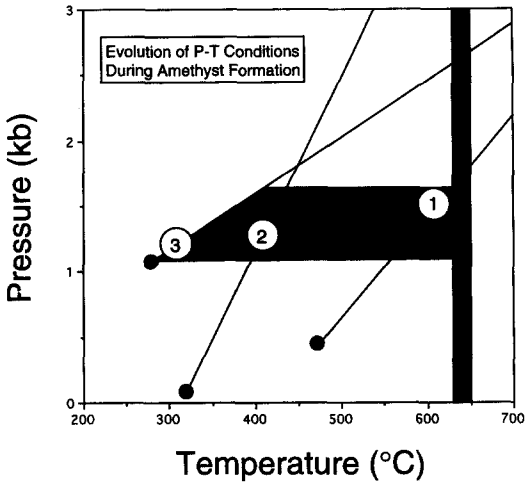

Fig. 7. Pressure-temperature diagram showing trapping conditions and fluid evolution involved during the formation of amethyst. The solidus temperature for the granites (630-670℃) is shown by the shaded rectangle (Yang, 1993). The isochore for type I liquid-rich inclusions with a salinity of 24 wt% and Th of 470℃ is labeled "1". The isochore for type II halite-bearing inclusions with a salinity of 34 wt% and Th of 320℃ is labelled "2". The isochore for type III CO_2-bearing inclusions with a salinity of 4 wt% and Th of 280℃ is labelled "3". The lightly shaded box represents the limits of temperature (650-280℃) and pressure (1.0-1.5 kbars) over which the amethyst could have formed, and the arrow suggests a possible P-T path during formation the of crystals.

the white quartz. Type I inclusions have salinities of about 24 wt.% NaCl equivalent and homogenization temperatures between 447 and 480℃ showing minimum trapping pressure at about 500 bars. Intermediate-aged quartz was precipitated from fluids represented by primary and/or pseudosecondary type II inclusions showing salinities of 33-34 wt.% NaCl equivalent and homogenization temperatures of 333°-320℃ showing minimum trapping pressure at about 150 bars. The latest generation of fluids is represented by type III H_2O-CO_2-NaCl inclusions found in the amethyst (the upper part of the quartz). Homogenization temperatures of type III inclusions are between 273°-288℃ with salinities of 4 wt.% NaCl equivalent showing minimum trapping pressure at about 1 kbar.

Based on the results of this study, the following evolution of P-T conditions during formation of the amethyst is proposed (Fig. 7). The similarity of the earliest inclusions in the white quartz base of the crystals with those associated with melt inclusions in the host granite suggests that the quartz began growing at near solidus conditions of the granite (Yang, 1993). The intersection of the isochore representing the early type I inclusions with the solidus temperature of 630° to 650℃ (Yang, 1993) indicates initial quartz formation at about 600℃ and 1.0 -1.5 kbars. Intermediate quartz formation associated with the high-salinity type II inclusions occurred at somewhat lower temperatures (~400℃) and pressures of about 1 kbar. The amethystine quartz formed from H_2O-CO_2-NaCl fluids at temperatures between about 280-400℃ and pressures of about 1 kbar.

The earlier interpretation (Youn and Park, 1994) suggesting that the amethyst deposits formed at low pressure was based on the assumption that the amethyst precipitated from boiling solutions. When fluid boils, it is simultaneously seperated into two groups; a very low-salinity fluid and a high-salinity. These two groups must show their spatial coexistence with the same homogenization temperatures when they are used as a boiling pair. Although liquid-rich (type I and II) inclusions in the quartz along with some vapor-rich (type IV) inclusions were observed, the two different types were never found to coexist in the same growth zone. Thus, it is suggested that the earlier evidence of boiling, which formed the basis of the earlier pressure determination, is somewhat ambiguous. If boiling fluids were associated with the amethyst, they were present after amethyst formation, apparently after much uplift and erosion and cooling had taken place. Moreover, the occurrence of H_2O-CO_2-NaCl inclusions in the outermost amethystine quartz requires a minimum pressure of about 1 kbar, based on the equations of state of Bowers and Helgeson (1983) (calculated using the program MacFlinCor;

Brown and Hagemann, 1994).

Mathane and nitrogen are recently reported by the introduction of micro-Raman analysis (Kerkhof and Thiery, 1994). It is reported that they are usually found in diagenetic and low-grade metamorphic rocks. Although the origin of these gases has not been clarified, they are assumed to be locally derived from organic matter of sedimentary origin based on the outcrop and microscopic observations. CO_2-bearing fluid is also assumed to be derived by the decabonization reactions (Yang *et al.*, 1994). Thus, early quartz is interpreted to have formed from fluids that either exsolved from or were in equilibrium with the granite at near solidus conditions, whereas the amethystine quartz apparently grew from fluids of at least partial sedimentary origin.

ACKNOWLEDGMENTS

I would like to thank Prof. Ahan J. H., Dr. Chi S. J. and the unknown reviewer for their comments of this paper. They have improved this paper considerably. Professor Bob Bodnar in the Virginia Tech is thanked for his critical comments and letting the author use his lab including Raman spectroscopy during summer visit in 1995. He always points out problems in ways that were not always immediately obvious to me.

REFERENCES

Bodnar, R. J., and Sterner, S. M., 1987, Synthetic Fluid inclusions: in G. C. Ulmer and H.L. Barnes, eds., Hydrothermal Experimental Techniques, Wiley- Interscience, New York, 423-457.

Bodnar, R. J., Burnham, C. W. and Sterner, S. M., 1985, Synthetic fluid inclusions in natural quartz. III. Determination of phase equilibrium properties in the system H_2O-NaCl to 1000℃ and 1500 bars. Geochim. Cosmochim. Acta, 49, 1861-1873.

Bodnar, R. J., Sterner, S. M. and Hall D. L., 1989, Salty: A Fortran program to calculate compositions of fluid inclusions in the system NaCl-KCl-H_2O. Computers & Geosciences, 15, 19-41.

Bodnar, R. J., and Vityk, M. O., 1994, Interpretation of microthermometric data for H_2O-NaCl fluid inclusions: in B. De Vivo and M. L. Frezzotti, eds., Fluid Inclusions in Minerals, Methods and Applications, Virginia Tech, Blacksburg, VA, 117-130.

Bowers, T. S. and Helgeson, H. C. 1983, Calculation of the thermodynamic and geochemical consequences of nonideal mixing in the system H_2O-CO_2-NaCl on phase relations in geologic systems: Equation of state for H2O-CO2-NaCl fluids at high pressures and temperatures. Geochim. Cosmochim. Acta, 47, 1247-1275.

Brown, P. E. and Hagemann, S. G., 1994, MacFlincor: A computer program for fluid inclusion data reduction and manipulation. in B. De Vivo and M.L. Frezzotti, eds., Fluid Inclusions in minerals, Methods and Applications Virginia Tech, Blacksburg, VA, 231-250.

Chang, K. H., 1975, Cretaceous stratigraphy of southeast Korea. J. Geol. Soc. Korea, 11, 1-23.

Darling, R. S., 1991, An extended equation to calculate NaCl contents from final clathrate melting temperatures in H_2O-CO_2-NaCl fluid inclusions: Implications for P-T isochore location. Geochim. Cosmochim. Acta, 55, 3869-3871.

Hall, D. L., Sterner, S. M. and Bodnar, R. J., 1988, Freezing point depression of NaCl-KCl-H_2O solutions. Economic Geology, 83, 197-202.

Hong, Y. K., 1987, Geochemical chracteristics of Precambrian, Jurassic and Cretaceous granites in Korea. J. Korea Inst. Mining Geol., 20, 35-60.

Jin, M. S., 1985, A relationship between tectonic setting and chemical composition of the Cretaceous granitic rocks in Southern Korea. J. Geol. Soc. Korea, 21, 67-73.

Jin, M. S., 1986, Geochemistry of the Cretaceous to early Tertiary granitic rocks in southern Korea. J. Geol. Soc. Korea, 21, 297-316.

Jin, M. S., Kim, S. Y. and Lee, J. S., 1981, Granitic magmatism and associated mineralization in the Gyeongsang Basin, Korea, Mining Geol., 31, 245-260.

Kerkhof, F. and Thiery, R., 1994, Phase transitions and density calculation in the CO_2-CH_4-N_2 system. in B. De Vivo and M. L. Frezzotti, eds., Fluid Inclusions in Minerals, Methods and Applications, Virginia Tech, Blacksburg, VA, 117-130.

Kim, J. J. and Moon, S., 1984, A study of fluid inclusion in Eonyang amethyst mine. J. of Sci., 38, Pusan National Univertsity, Pusan, Korea, 263-274.

Kim, W., Shin, H., and Lee, S., 1988, Characterization of inclusions in amethysts from Eonyang, Korea. J. Min. Soc. Korea, 1, 83-93.

Lee, S. M., 1972, Granites and mineralization in Gyeongsang Basin (in Korean). Memoirs in celebration of the 60th birthday of prof. C. M. Son, 195-220.

Lee, S. M., Kim, S. W., and Jin, M. S., 1987, Igneous activities of the Cretaceous to the early Tertiary and their tectonic implication in South Korea (in Korean). J. Geol. Soc. Korea, 23, 338-359.

Lee, Y. J. and Ueda, Y., 1976, K-Ar dating on granitic rocks from the Eonyang and the northwestern part of Ulsan-quadrangle, Kyeongsang- nam-do, Korea. J. Korea. Inst. Min. Geol., 9, 123-130.

Min, K. D., Kim, O. J. Yun. S. K., Lee, D. S., and Joo, S. W., 1982, Applicability of plate tectonics to the post-late Cretaceous igneous activities and mineralization in the southern part of South Korea (I) (in Korean). J. Korean Inst. Mining Geol., 15, 123-154.

Yang, K., 1993, Fluid inclusions from the Cretaceous-early Tertiary granitoids in the southeastern Gyeongsang Basin, Korea, Unpub. Ph. D. Dissertation, Pusan National University, Pusan, Korea.

Yang, K., Kim, S., and Kim, J. J., 1994, Fluid inclusion study of the amethyst and related granites in the Eonyang amethyst mining district. J. Geol. Soc. Korea, 30, 591-601.

Youn, S. T. and Park, H. I., 1994, A study on the genesis of Eonyang amethyst deposit. Econ. Environ. Geol., 27, 335-343.

(책임편집 : 안중호)

언양 자수정 형성 환경의 압력-온도-성분에 대한 유체포유물의 이용

양 경 희

부산대학교 자연과학대학 지질학과

요 약 : 언양 자수정 광상은 경상분지의 백악기 말-고 제 3기 화강암과 시공간적으로 관련성을 가진다고 여겨져왔다. 흑운모 화강암을 관입한 애플라이트내에 발달한 정동내에 자형의 석영이 저면에서는 백색, 상부에서는 자주색을 띠며 산출되어진다. 3 형태의 초생 포유물이 관찰 되어졌고, 자수정이 성장한 환경과 유체의 진화에 대한 조사를 위해 이 3 형태에 따른 3개의 아이스코아가 만들어졌다. 모암의 고상선 온도와 초기 포유물의 아이스코아의 교점에 의해, 최초의 석영은 약 600℃, 1.0-1.5 kbars에서 자라기 시작했다. 중간단계의 석영은 400℃정도, 1 kbar에서 염도가 높은 열수에서, 자수정은 280-400℃, 1 kbar에서 H_2O-CO_2-NaCl 열수에서 만들어졌다. 초기에 형성된 석영은 마그마의 고상선 환경부근에서 화강암에서 용리 되어졌거나, 혹은 화강암과 평형을 이루고 있었던 열수에서 만들어졌으며, 자수정은 적어도 부분적으로 퇴적 기원을 가진 유체에서 성장했다.

핵심어 : 초생포유물, 포획환경, 아이스코아